Journal of Environmental Chemical Engineering 9 (2021) 106357

Contents lists available at ScienceDirect

Journal of Environmental Chemical Engineering

journal homepage: www.elsevier.com/locate/jece

Imidazolium-based cationic polymeric nanotraps for efficient removal of $Cr_2O_7^{2-}$

Xiaorui Li [a], Linfeng Jin [b], Lei Huang [c], Xueying Ge [d], Haoyu Deng [a], Haiying Wang [a,e,g], Yiming Li [f,*], Liyuan Chai [a,e,**], Shengqian Ma [d,*]

[a] School of Metallurgy and Environment, Central South University, Changsha, Hunan 410083, China
[b] School of Material Science and Engineering, Central South University, Changsha, Hunan 410083, China
[c] School of Environmental Science and Engineering, Guangzhou University, Guangzhou, Guangdong 510006, China
[d] Department of Chemistry, University of North Texas, Denton, TX 76201, USA
[e] Chinese National Engineering Research Center for Control & Treatment of Heavy Metal Pollution, Changsha, Hunan 410083, China
[f] College of Chemistry and Chemical Engineering, Central South University, Changsha, Hunan 410083, China
[g] Water Pollution Control Technology Key Lab of Hunan Province, Changsha, Hunan 410004, China

ARTICLE INFO

Editor: Yunho Lee

Keywords:
Cationic polymeric nanotraps
$Cr_2O_7^{2-}$ removal
Influence of counterion
Wettability
Counter anion exchange

ABSTRACT

Two imidazolium-based cationic polymeric nanotraps based on tetraphenylmethane building blocks (CPN-tpm) with different counterions were rationally designed and constructed for the efficient removal of $Cr_2O_7^{2-}$ from wastewater. The influence of counterions on $Cr_2O_7^{2-}$ adsorption performance was studied. With better wettability (contact angle as 28.61°), CPN-tpm-Cl exhibited a higher uptake capacity of 366 mg g^{-1} for $Cr_2O_7^{2-}$ capture and a faster ion exchange kinetic process in 20 min. While CPN-tpm-Br with a contact angle of 83.16° showed a lower maximum capacity of 324 mg g^{-1}. In addition, CPN-tpm-Cl can work in a wide pH range from 2 to 10 and possess excellent selectivity (such as Cl^-, NO_3^- and SO_4^{2-}) as well as good reusability for 5 times. Such excellent performances indicated that CPN-tpm-Cl is a promising candidate for the $Cr_2O_7^{2-}$ capture application. Our work not only contributes cationic polymeric nanotraps as a promising candidate for $Cr_2O_7^{2-}$ removal, but also suggests a new approach to develop new type of adsorbents for wastewater treatment.

1. Introduction

Hexavalent chromium has been widely used in a variety of industries such as printing, electroplating, leather tanning, steel manufacturing, textile dying and so on [1–3]. Moreover, hexavalent chromium is found to be highly toxic, teratogenic and potentially carcinogenic to living systems, even at low concentration. Many efforts have been dedicated to removing Cr(VI) from wastewater and different types of adsorbents have been developed, such as inorganic materials [4], composites [5], activated carbon [6], cationic polymers [7,8], MOFs [9–11] and so on. However, disadvantages such as slow kinetic process, low uptake capacity and poor stability of materials hampered their application in practice. Thus, it is of great importance and urgent need to develop new types of efficient adsorbents for Cr(VI) removal.

In the past decade, cationic polymers have emerged as a versatile platform for applications in many fields, such as gas sorption and separation [12,13], catalysis [14,15], batteries [16], ion detection [2] and adsorption [17,18], due to the positive charges incorporated in the skeleton and exchangeable counterions residing in cavities [19]. Meanwhile, the properties of cationic polymers can be easily tuned by changing the counterions for desired applications, such as catalysis [20], CO_2 adsorption and conversion [21], electrolytes [22], and so on. Furthermore, counterion adjustment is an effective and convenient approach to modify the wettability of the material surface, which helps improving the polymer dispersity in water and facilitating the kinetic exchange process in aqueous condition [23]. Such modification could make cationic polymers the ideal candidate for pollutants removal in wastewater.

Herein, two tetraphenylmethane-based cationic polymeric nanotraps with different counterions (CPN-tpm-Cl and CPN-tpm-Br) were prepared and compared for the removal of $Cr_2O_7^{2-}$, as one of the most common Cr (VI) form in water. In the design, positively charged imidazolium groups

* Corresponding authors.
** Corresponding author at: School of Metallurgy and Environment, Central South University, Changsha, Hunan 410083, China.
E-mail addresses: chemyl@csu.edu.cn (Y. Li), lychai@csu.edu.cn (L. Chai), Shengqian.Ma@unt.edu (S. Ma).

https://doi.org/10.1016/j.jece.2021.106357
Received 25 July 2021; Received in revised form 3 September 2021; Accepted 7 September 2021
Available online 11 September 2021

play an important role in anion capture, while tetraphenylmethane (tpm) average these charges spatially and reduce the repulsion from neighbor counterions. Benefiting from the cationic structure, such nanotraps exhibited good adsorption performance for $Cr_2O_7^{2-}$ capture. Moreover, to study the influence of different counterions between Br^- and Cl^-, Raman spectroscopy, XPS, FTIR and other techniques were used to investigate the ion exchange mechanism for $Cr_2O_7^{2-}$ capture.

2. Materials and methods

2.1. General

1,4-bis(bromomethyl)benzene was purchased from Acros Organics. Potassium dichromate ($K_2Cr_2O_7$), sodium chloride (NaCl), sodium hydroxide (NaOH), and hydrochloric acid (HCl) were purchased from Sinopharm Chemical Reagent Co., Ltd, China. The syringe filters (Nylon 66, 0.45 μm) were purchased from Jinlong company, China. $Cr_2O_7^{2-}$ solutions were prepared by dissolving certain amounts of potassium dichromate in distilled water. The pH values were adjusted by sodium hydroxide or hydrochloric acid.

2.2. Synthesis methods

CPN-tpm-Br was synthesized from tetrakis[4-(1-imidazolyl)phenyl] methane [24] (1.0 equiv.) and 1,4-bis(bromomethyl)benzene (1.0 equiv.). The mixture was stirred in DMF at 120 °C under N_2 for 12 h and precipitate was formed. After filtration, the solid was washed 3 times with DMF, deionized water and ethanol subsequently. Then the product was dried in a vacuum oven to obtain CPN-tpm-Br.

2.3. Characterization methods

Scanning electron microscopy (SEM) images were obtained from a MIRA3 LMH (TESCAN, Czech Republic) and elemental mapping images were obtained by X MAX20 (Oxford, UK). Thermal gravimetric analysis (TGA) was carried out using a NETZSCH STA449F3 Jupiter thermogravimetric analyzer at a heating rate of 10 K min^{-1} in Ar atmosphere (NETZSCH, Germany). Water vapor adsorption–desorption isotherm at 298 K were measured using Micromeritics ASAP 2020 M and Tristar system. And before the measurements, the sample was outgassed for 1000 min at 120 ℃. The data of Zeta potential was detected using Malvern Zano-zs and the data of size distribution report was measured by Malvern Zetasizer Nano ZS90. The concentration of $Cr_2O_7^{2-}$ was detected by UV-Vis spectra (U-4100, HITACHI, Japan). Fourier transform infrared (FTIR) spectra were recorded with FTIR spectrometer (Nicolet IS10, Thermo scientific, USA) by mixing samples with KBr powder to form pellets. X-ray photoelectron spectroscopy (XPS) experiments were conducted on a Thermo ESCALAB Xi+ analyzer (Thermo Fisher Scientific Inc., USA) with Al Kα radiation ($hv = 1486.6$ eV) as the excitation source, and the binding energies were calibrated using the C 1s peak at 284.80 eV. The contact angles experiments of water were performed on a contact angle measuring instrument (XG-CAMC1). Raman spectroscopy was carried out using a inVia Raman Microscope (RENISHAW, UK), and a 785 nm semiconductor laser was used as the excitation source.

2.4. Sorption general procedures

All batch experiments were conducted in a water-bathing vibrator at 30 ℃. The pH values were adjusted by NaOH or HCl aqueous solution. CPN-tpm-Cl or CPN-tpm-Br was added into a certain concentration of $Cr_2O_7^{2-}$ aqueous solution in the flask. After shaking at a rate of 120 rpm for a desired period, the mixture was separated with a membrane filter (0.45 μm). The filtrate was monitored by the UV-Vis spectroscopy at 257 nm [10].

2.5. pH effect study

Effect of pH on the adsorption properties of $Cr_2O_7^{2-}$ was tested by adjusting pH values from 0 to 12. 5 mg of CPN-tpm-Cl and CPN-tpm-Br was added to 10 mL of $Cr_2O_7^{2-}$ aqueous solution with a concentration of 100 ppm (V/m ratio is 2000 mL g^{-1}). After shaking for 4 h, the mixture was separated for UV-Vis analysis.

2.6. Sorption isotherm investigations

The sorption isotherm experiments of CPN-tpm-Cl and CPN-tpm-Br were carried out by ranging the initial concentrations of $Cr_2O_7^{2-}$ from 10 to 500 ppm. 5 mg of CPN-tpm-Cl or CPN-tpm-Br was added to $Cr_2O_7^{2-}$ aqueous solution (10 mL) with different concentrations (V/m ratio is 2000 mL g^{-1}). After shaking for 4 h, the mixture was separated with a membrane filter for UV-Vis analysis. Adsorption capacity at equilibrium q_e (mg g^{-1}) was calculated by Eq. 1.

$$q_e = \frac{(C_0 - C_e) \times V}{m} \tag{1}$$

Where C_0 (mg L^{-1}) and C_e (mg L^{-1}) are the concentration of $Cr_2O_7^{2-}$ at initial time and equilibrium time, respectively. m is the mass of CPN-tpm-Cl/Br (g) and V (L) is the volume of $Cr_2O_7^{2-}$ solution.

The Langmuir isotherm model is an ideal model with monolayer sorption on a homogeneous surface and adsorption sites of equal energy on the assumption [17]. And the Langmuir isotherm model can be expressed as Eq. 2.

$$\frac{C_e}{q_e} = \frac{C_e}{q_m} + \frac{1}{K_L \times q_m} \tag{2}$$

Where q_e (mg g^{-1}) and q_m (mg g^{-1}) are sorption capacity of $Cr_2O_7^{2-}$ at equilibrium and maximum sorption capacity of $Cr_2O_7^{2-}$, respectively. C_e (mg L^{-1}) is the equilibrium concentration of $Cr_2O_7^{2-}$. K_L (L mg^{-1}) is a constant related to the affinity between the adsorbate and adsorbent.

The Freundlich isotherm model is an empirical model which assumes a heterogeneous surface with adsorption sites of different adsorption energies. And the Freundlich isotherm model can be expressed to Eq. 3 as follows.

$$\ln q_e = \ln K_F + \frac{1}{n} \ln C_e \tag{3}$$

Where K_F [(mg g^{-1}) (L g^{-1})^n] and is a constant which indicates the adsorption capacity, and n is a heterogeneity constant related to the adsorption intensity.

2.7. Sorption kinetics investigations

The sorption kinetics experiments of CPN-tpm-Cl and CPN-tpm-Br were conducted by collecting samples at different times. 15 mg of CPN-tpm-Cl and CPN-tpm-Br was added to 100 mL of $Cr_2O_7^{2-}$ aqueous solution (the initial concentration is 50 ppm) in a 250 mL Erlenmeyer flask (V/m ratio is 6.67 $\times 10^3$ mL g^{-1}). The flask was put in the water-bathing vibrator and shaken at a rate of 120 rpm. Then samples with the volume of 2 mL were removed from the mixture at increasing time intervals (1 min, 2 min, 3 min, 5 min, 10 min, 15 min, 20 min, 30 min, 60 min, 900 min), followed by separation with a membrane filter (0.45 μm) for further analysis.

Removal efficiency (RE) is calculated by Eq. 4.

$$RE = \frac{C_0 - C_t}{C_0} \times 100\% \tag{4}$$

Where C_0 (mg L^{-1}) and C_t (mg L^{-1}) are the concentration of $Cr_2O_7^{2-}$ at initial time and t (min), respectively.

There are a lot of equations to fit sorption kinetics data, pseudo-first-order model and pseudo-second-order model are widely used among

them [25]. Pseudo-first-order linear equation and pseudo-second-order linear equation are expressed to Eq. 5 and Eq. 6, respectively.

$$\ln(q_e - q_t) = \ln q_e - k_1 t \quad (5)$$

$$\frac{t}{q_t} = \frac{1}{k_2 \times q_e^{\,2}} + \frac{t}{q_e} \quad (6)$$

Where q_t (mg g^{-1}) and q_e (mg g^{-1}) are sorption capacity of $Cr_2O_7^{2-}$ at a desired time t (min) and equilibrium time, respectively. k_1 (min^{-1}) and k_2 (g mg^{-1} min^{-1}) are the constants of pseudo-first-order model and pseudo-second-order model, respectively.

2.8. Selectivity study

Effect of competing ions was investigated by adding different concentrations of NaCl, $NaNO_3$ and Na_2SO_4, respectively. 5 mg of CPN-tpm-Cl was added to 10 mL $Cr_2O_7^{2-}$ solution (100 ppm, 0.463 mM, V/m ratio is 2000 mL g^{-1}) with different concentrations of Cl^-, NO_3^- and SO_4^{2-} (0.463 mM, 2.315 mM, 4.63 mM). After shaking at 30 °C for 15 h, the mixture was separated for UV-Vis analysis.

2.9. Reusability study

The adsorption-desorption process for 5 times was conducted to test the reusability of the polymer. 50 mg CPN-tpm-Cl was adsorbed with 50 mL $Cr_2O_7^{2-}$ solution (100 ppm) at constant temperature 30 °C for 1 h (V/m ratio is 1000 mL g^{-1}). Then CPN-tpm-Cr was regenerated by 2 M NaCl solution of 10 mL at 30 °C. And the process was repeated for additional four times of adsorption-desorption test.

3. Results and discussion

3.1. Characteristics

The aforementioned CPN-tpm-Br was synthesized with tetrakis[4-(1-imidazolyl)phenyl]methane and 1,4-bis(bromomethyl)benzene in dimethylformamide (DMF) at 120 °C [24]. Solid-state ^{13}C NMR was performed to verify the structure of the polymer. From Fig. S1, C1 and C6 were assigned to the central carbon atom of tetraphenylmethane and the carbon atoms in imidazolium rings, respectively. And C11 was attributed to carbon atoms of methylene in 1,4-bis(bromomethyl)benzene. All of the peaks were fully assigned. Furthermore, the broad peaks instead of sharp ones in the NMR spectrum indicated successful synthesis of the polymeric structure. In addition, from FT-IR spectrum (Fig. 9b), the characteristic peak at 1072 cm^{-1} was attributed to quaternary imidazolium species indicative of the formation of CPN-tpm with positive charges. The anion exchange process of CPN-tpm was shown in Scheme 1. The counterion exchange from Br^- to Cl^- was achieved by soaking CPN-tpm-Br in 2 M sodium chloride solution for three times and dried in the vacuum oven. The morphology of synthesized cationic polymers was characterized by SEM technique. As shown in Fig. 1a and b, the full spheres with diameter around 2.5 μm were observed in the SEM images of CPN- tpm-Br and CPN-tpm-Cl, and the size distribution of CPN-tpm-Cl was conducted and shown in Table S1 (see ESI). Although the morphologies of CPN-tpm-Cl and CPN-tpm-Br are quite similar, their air-water contact angles on the surface are very different (28.61° for CPN-tpm-Cl and 83.16° for CPN-tpm-Br in Fig. 1c and d). Therefore, the anion exchange process from Br^- to Cl^- significantly improved the surface hydrophilicity of the cationic polymeric nanotraps [24]. Furthermore, the water vapor adsorption experiment (Fig. 2) showed that CPN-tpm-Cl had a remarkable water vapor uptake with the maximum capacity up to 295 cm^3 g^{-1} (23.7 wt%) when P/P_0 is 0.71. When P/P_0 is below 0.1, there is a rather steep uptake which can be presumably ascribed to its hydrophilic nature due to imidazole group with positive charge [26,27]. These results indicated that the counterion adjustment could improve the surface hydrophilicity. From the curves in Fig. S2 (see ESI), thermogravimetric analysis was also conducted and both CPN-tpm-Br and CPN-tpm-Cl had the similar decreasing trend, and were stable up to 230 °C. In addition, their initial weight losses below 150 °C were mainly originated from the removal of the solvent molecules [28].

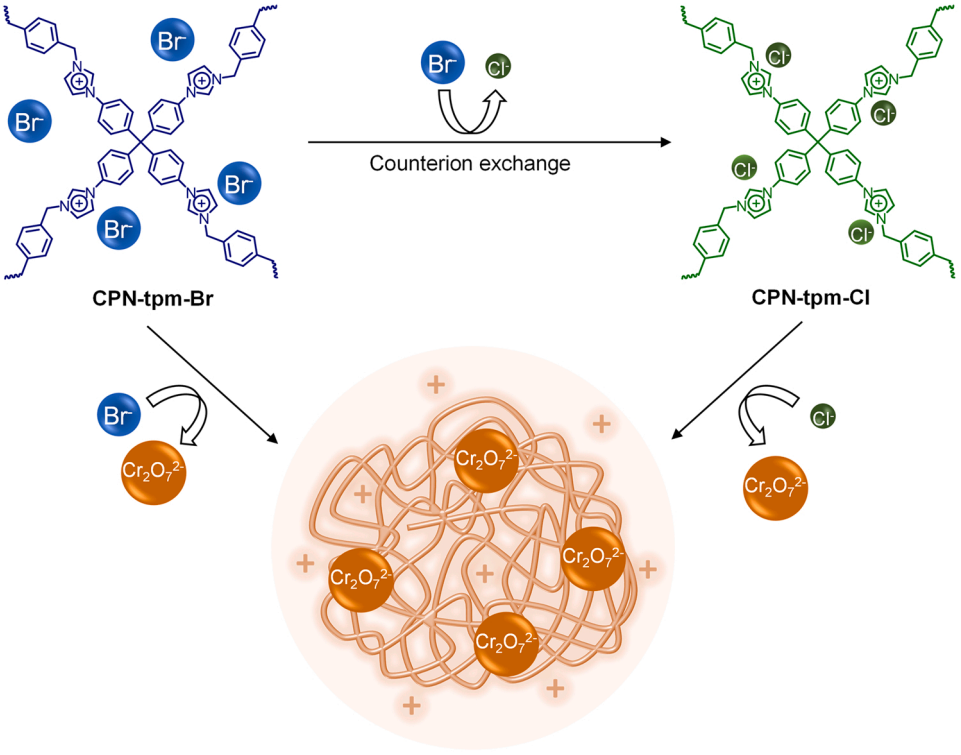

Scheme 1. Anion-exchange process of CPN-tpm.

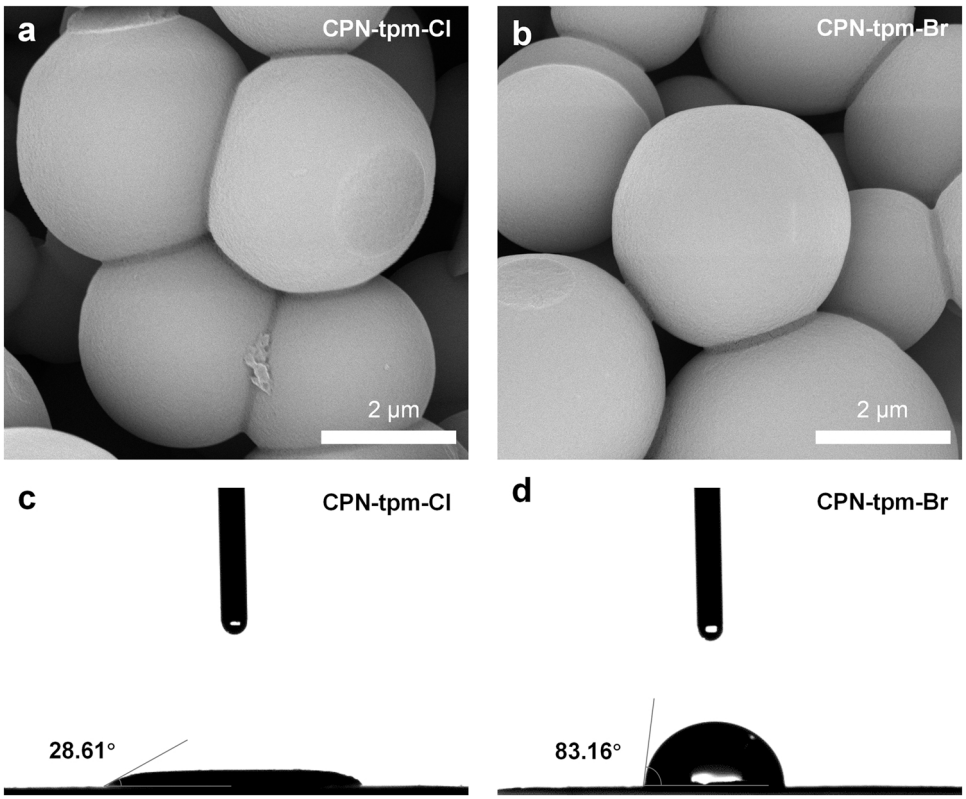

Fig. 1. SEM images of a) CPN-tpm-Cl and b) CPN-tpm-Br. Contact angle measurements for c) CPN-tpm-Cl and d) CPN-tpm-Br.

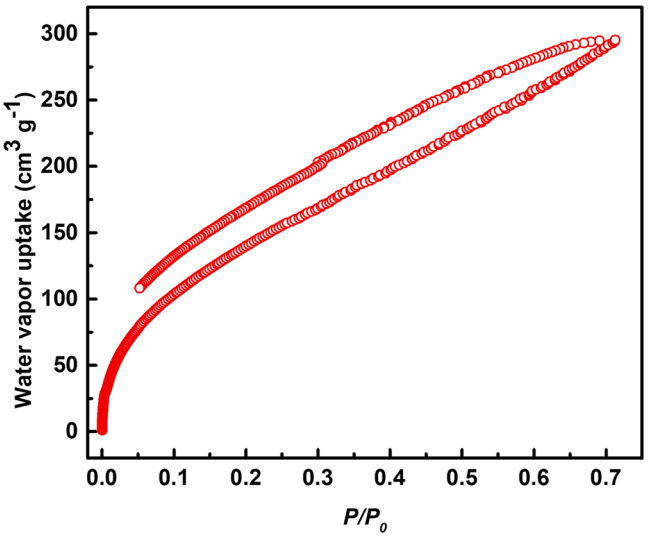

Fig. 2. Water vapor adsorption–desorption isotherm of CPN-tpm-Cl at 298 K, P_0 is the saturated vapor pressure of water vapor.

3.2. Anion exchange performance

Given the polymers built by cationic imidazolium units, the capacities of CPN-tpm for $Cr_2O_7^{2-}$ adsorptions were studied with $K_2Cr_2O_7$ solution. After 5 mg CPN-tpm-Cl was dispersed in aqueous $Cr_2O_7^{2-}$ solution (100 ppm, 10 mL) for 2 min (V/m ratio is 2×10^3 mL g^{-1}), the filtrate was monitored by the UV-Vis spectroscopy at 257 nm to inspect the adsorption of $Cr_2O_7^{2-}$ [10]. As shown in Fig. 3a, the residual $Cr_2O_7^{2-}$ concentration was decreased sharply by 91.3%. In two minutes, the color of $Cr_2O_7^{2-}$ solution was changed from yellow to colorless, while the adsorbent of CPN-tpm-Cl was turned from white to yellow (inset of Fig. 3a).

To further test the adsorption performance towards $Cr_2O_7^{2-}$ and investigate the influence of hydrophilicity difference brought by different counterions, the experiments of pH tolerance, adsorption isotherm and adsorption kinetics were conducted. 5 mg of CPN-tpm-Cl or CPN-tpm-Br was dispersed respectively in 10 mL $Cr_2O_7^{2-}$ aqueous solution with different pHs from 0 to 12 (V/m ratio is 2000 mL g^{-1}) to test the pH tolerance. As we can see in Fig. 3b, in the pH range from 2 to 6, the removal efficiencies of $Cr_2O_7^{2-}$ were over 95% for both CPN-tpm-Cl and CPN-tpm-Br. Interestingly, different from CPN-tpm-Br, cationic polymer with Cl^- keeps high removal uptake in a wider pH range (from 2 to 10), which can be applied easily in the actual wastewater. At pH 0, the removal efficiency was decreased rapidly due to the existence of excess Cl^- ions in the solution and their competition with $Cr_2O_7^{2-}$, since the molar ratio between Cl^- and $Cr_2O_7^{2-}$ has reached 2160:1 at such low pH. Nevertheless, even under such high ionic concentration, the removal percentage of CPN-tpm-Cl for $Cr_2O_7^{2-}$ can still maintain as high as 57.8%. At pH 2, both CPN-tpm-Cl and CPN-tpm-Br can remove almost all Cr-contained pollutants in water, which is competent for acidic wastewater. In addition, most of Cr species in industrial waste existed under acidic conditions, but in some circumstances, such as in the groundwater, they were also observed in the alkaline or neutral environment [29,30]. To further investigate the adsorption performance at high pH value, Zeta Potential test was conducted in neutral solution and weak alkaline solution [31]. According to the result (Table S2) and previous report [24], CPN-tpm exhibited positive values with a wide pH range from 1 to 12, indicating that the surface of CPN-tpm was positively charged and kept effective for the capture of anionic pollutions in a wide pH range [18]. Additionally, the stability of polymer was tested by soaking polymers in acidic (pH 2) and alkaline (pH 12) solutions for 8 h and IR spectra were conducted. From Fig. S3, the result showed that CPN-tpm-Cl, CPN-tpm-Cl-pH 2 and CPN-tpm-Cl-pH 12 have the similar characteristic peaks, indicating that CPN-tpm has good stability in acidic and alkaline conditions.

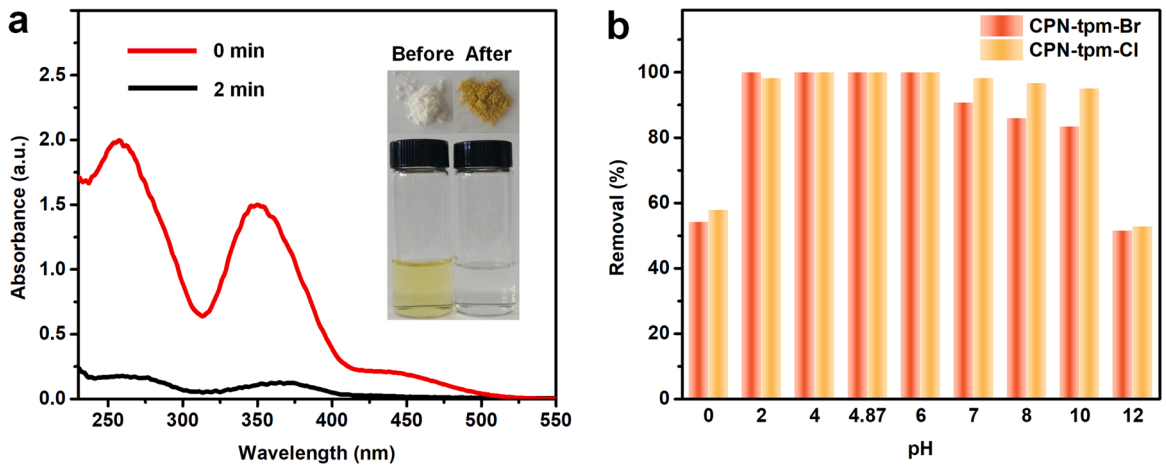

Fig. 3. a) UV-Vis spectra of aqueous $K_2Cr_2O_7$ solution before and after chromium removal using CPN-tpm-Cl, inset are photos showing color changes of the solution and materials before and after chromium uptake. b) Comparison of sorption properties of $Cr_2O_7^{2-}$ by CPN-tpm-Br and CPN-tpm-Cl at different pH. (For interpretation of the references to color in this figure legend, the reader is referred to the web version of this article.)

In order to investigate the adsorption kinetics of the polymer networks, UV-Vis spectrometry was employed. In Fig. 4a and b, 15 mg of CPN-tpm-Cl and CPN-tpm-Br were separated in 50 ppm $Cr_2O_7^{2-}$ aqueous solution and UV adsorption was tested at different times for kinetic analysis (V/m ratio is 6.67×10^3 mL g^{-1}). After adding CPN-tpm-Cl and CPN-tpm-Br, decreases of $Cr_2O_7^{2-}$ concentration were clearly observed. Interestingly, the kinetics between CPN-tpm-Br and CPN-tpm-Cl are quite different as indicated from the curves of 1 min. Until 30 min, the equilibrium concentration of CPN-tpm-Br can reach the same level as that of CPN-tpm-Cl at 1 min. The result showed that CPN-tpm-Cl can remove 93.0% of $Cr_2O_7^{2-}$ in the first 10 min, while it's only 52.2% for CPN-tpm-Br during the same time period. We speculated the faster kinetic of CPN-tpm-Cl was benefited from the smaller anion size and larger decoupling degree of Cl^- ion [32], which lead to a better binding affinity with solvent molecules and a faster ion exchange process. Furthermore, the half Br^- replaced sample was prepared and the kinetics was tested. From Fig. S4, the time-dependent UV-Vis adsorption curves showed a fast ion exchange process in the first few minutes; while after a few minutes, the ion exchange process slowed down. Such results further demonstrated the influence of counterions in the cationic polymers. As shown in Fig. 5a, the sorption equilibrium was reached within 20 min (95.8%), indicating a faster sorption process than CPN-tpm-Br. It is worth noting that such kinetic is also faster than many of previously reported ionic materials including UiO-66-NH_2@silica (30 min), TJNU-243 (8 h), 1-Br (48 h), $[Cu_2L(H_2O)_2]\cdot(NO_3)_2\cdot 5.5H_2O$ (100 min), CON-1 (60 min), IMIP-Br (30 min), as shown in Table S3. In addition, the fitting results of kinetic parameters are shown in Table S4 (see ESI). From inset of Figs. 5a and S5 in ESI, the sorption kinetics of CPN-tpm-Cl and CPN-tpm-Br towards $Cr_2O_7^{2-}$ can be better fitted with pseudo-second-order model, yielding a high correlation coefficient ($R^2 > 0.99$), indicating that chemical adsorption is likely the rate-determining step of ion exchange process between CPN-tpm with counterions (such as Br^- or Cl^-) and $Cr_2O_7^{2-}$ [33,34]. On the other hand, CPN-tpm-Cl can be dispersed in water easier than CPN-tpm-Br since CPN-tpm with Cl^- showed a better hydrophilicity, which may also contribute to the faster kinetics process.

In addition, the residual $Cr_2O_7^{2-}$ solutions were analyzed by UV-Vis spectrometer and the maximum adsorption capacities of CPN-tpm-Br and CPN-tpm-Cl were investigated. Moreover, sorption isotherm experiments of CPN-tpm with Br^- and Cl^- for $Cr_2O_7^{2-}$ were conducted by ranging the initial concentration of $Cr_2O_7^{2-}$ from 10 to 500 ppm (Fig. 5b). Langmuir isotherm model (Fig. S6) and Freundlich isotherm model (Fig. S7) were applied to fit the experimental data. Due to a higher correlation coefficient ($R^2 > 0.99$), the Langmuir isotherm model of two cationic polymers can fit better than the Freundlich isotherm model (Table S5). Furthermore, both CPN-tpm-Cl and CPN-tpm-Br showed high affinity to Cr-contained anions, and according to the experimental data, the maximum sorption capacity of CPN-tpm-Cl towards $Cr_2O_7^{2-}$ was 366 mg g^{-1}, higher than 324 mg g^{-1} of CPN-tpm-Br. According to previous reports (Table S3, ESI), such sorption capacity is

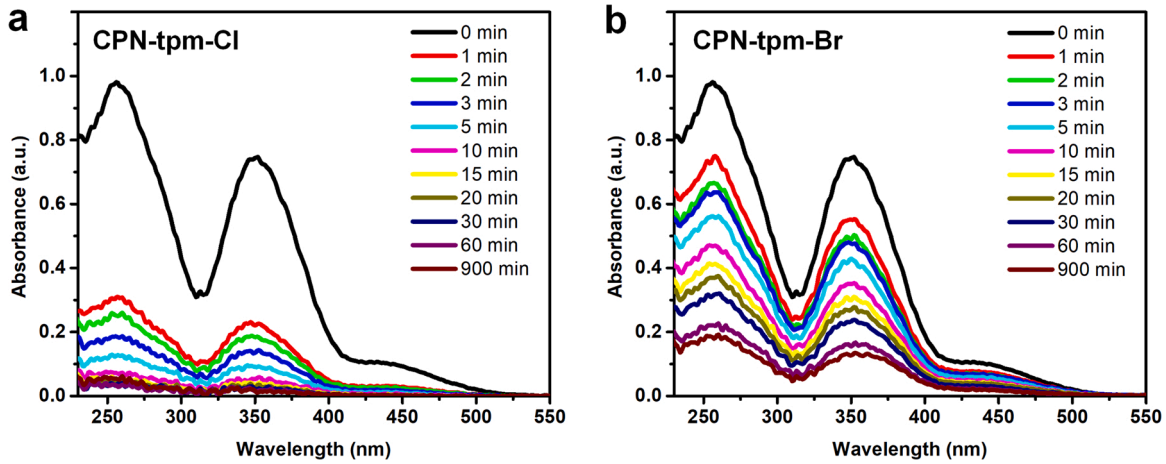

Fig. 4. a) Time-dependent UV-Vis adsorption curves of CPN-tpm-Cl. b) Time-dependent UV-Vis adsorption curves of CPN-tpm-Br.

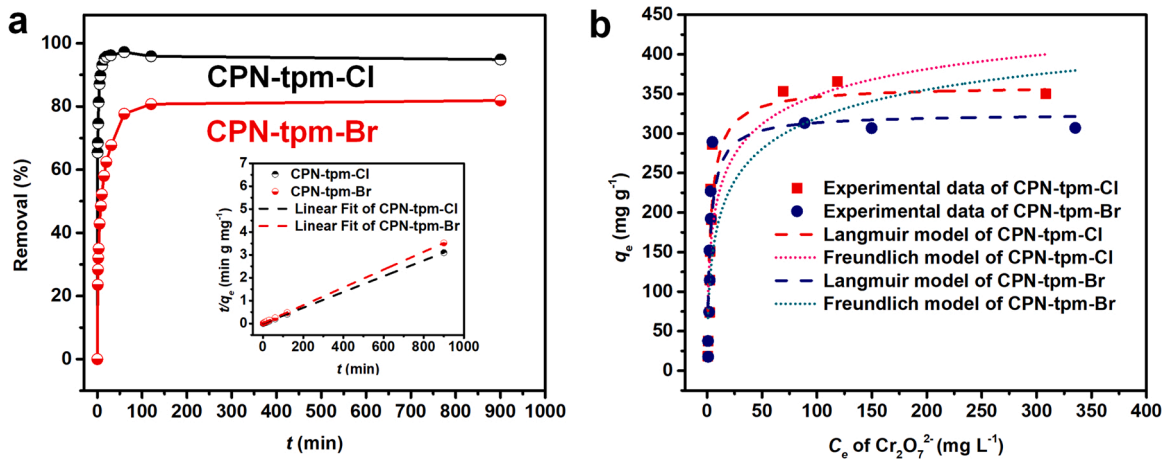

Fig. 5. a) Sorption kinetics of CPN-tpm-Cl and CPN-tpm-Br, and inset is the fitting curve based on the pseudo-second-order model. b) Sorption isotherm of CPN-tpm-Cl and CPN-tpm-Br for $Cr_2O_7^{2-}$ uptake.

much higher than most of the cationic materials [2,7–9,11,35]. We reasoned that such excellent sorption capacity towards $Cr_2O_7^{2-}$ should benefit from the 3D tetraphenylmethane backbone with imidazolium moieties, which provide dispersive positive charges for ion exchange between $Cr_2O_7^{2-}$ and counter anions.

Effect of competing ions (such as Cl^-, NO_3^- and SO_4^{2-}) on the removal rate of $Cr_2O_7^{2-}$ were conducted. As shown in Fig. 6a, even the molar ratios of Cl^-, NO_3^- and SO_4^{2-} were ten times in excess in the $Cr_2O_7^{2-}$ solution, the removal percentages for $Cr_2O_7^{2-}$ still remained as 95.5%, 94.2% and 90.0%, respectively (V/m ratio is 2000 mL g^{-1}). The high selectivity may result from the strong affinity between the $Cr_2O_7^{2-}$ and cationic imidazolium group in the skeleton of polymer. When the molar ratio between SO_4^{2-} and $Cr_2O_7^{2-}$ is 10:1, a slight decrease in removal rate suggested that the anions with more negative charges will have a stronger competition for $Cr_2O_7^{2-}$ adsorption.

Reusability of the cationic polymer is an essential factor for the evaluation of anion exchange process and the adsorption-desorption tests were performed for 5 times. As shown in Fig. 6b, the result showed the removal rate remained almost unchanged (over 98%) in first four runs. A slight decrease in the last run (87%) may due to the loss of material during the process of experimental operation. Integrating with good performances of anion exchange, CPN-tpm is a promising candidate for Cr-contained industrial wastewater.

3.3. Mechanism

The ion exchange mechanism was explored by SEM-EDX mapping, FT-IR, XPS analysis and Raman spectroscopy. As we can see in Fig. 7, after ion exchange from Br^- to Cl^-, the binding energy of N atoms in imidazolium ($IM\text{-}N^+$) deceased from 401.8 eV to 401.7 eV, indicating a

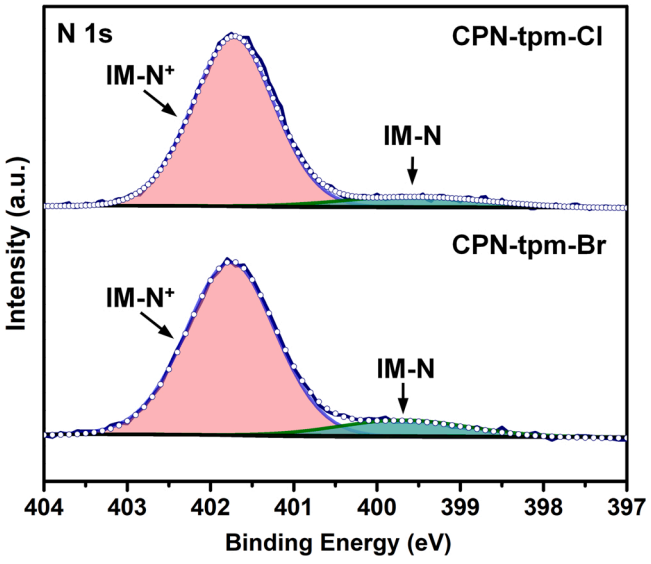

Fig. 7. N 1s core-level spectra of CPN-tpm-Cl and CPN-tpm-Br.

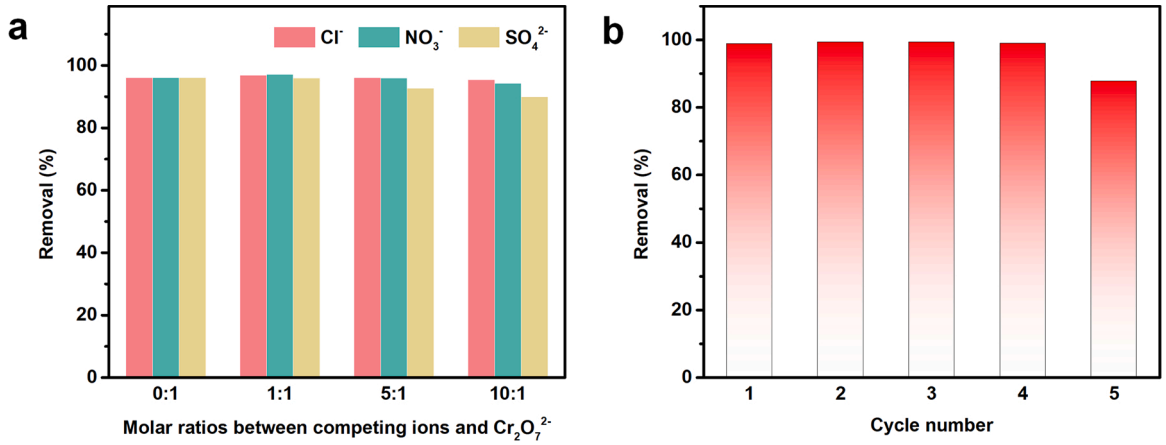

Fig. 6. a) Effect of competing anions (Cl^-, NO_3^- and SO_4^{2-}) on the removal of $Cr_2O_7^{2-}$. b) Reversibility of CPN-tpm-Cl for collecting $Cr_2O_7^{2-}$.

weaker interaction between imidazolium ring and Cl^- [36]. We speculate that with a smaller ionic radius and higher electron density, Cl^- has a weaker interaction with imidazolium group compared to Br^-, leading to a faster kinetic process and complete ion exchange equilibrium [37]. In Fig. 8, the SEM-EDX mapping of CPN-tpm before and after $Cr_2O_7^{2-}$ sorption showed that the abundances of Cl element and Br element were decreased and the abundance of Cr element emerged obviously in CPN-tpm-Cl-Cr and CPN-tpm-Br-Cr. Furthermore, after the anion exchange process, Cl residual can be barely observed in CPN- tpm-Cl-Cr. This indicates that the complete $Cr_2O_7^{2-}$ anion exchange process exists between Cl^- and $Cr_2O_7^{2-}$ (Fig. S8, see ESI). Furthermore, as shown in Fig. 9a, the presence of obvious Cr 2p peaks (576.8 eV) can be found on CPN-tpm-Br-Cr and CPN-tpm-Cl-Cr, indicating the Cr species on the surface of the CPN-tpm after sorption experiments. In addition, a new peak at 912 cm^{-1} can be attributed to Cr-O stretching in the FTIR spectra of CPN-tpm-Cl-Cr (Fig. 9b) [2,38–40]. Besides, the peaks at 1072 cm^{-1} were attributed to quaternary imidazolium moieties, which showed that the cationic functional group can still be observed after adsorption. Furthermore, in the Raman spectra of CPN-tpm-Cl-Cr and CPN-tpm-Br-Cr, the peaks around 900 cm^{-1} correspond to the Cr(VI)-O band frequency shifts [41], indicating the successful Cr species capture by the materials (Fig. 9c and d). Additionally, from the Fig. S9, it can be seen that CPN-tpm with different counterions before and after the adsorption could maintain the morphology, which indicated the stability of the cationic polymers during Cr removal process.

4. Conclusion

In conclusion, we have demonstrated the construction of imidazolium-based cationic polymeric nanotraps using a custom-designed building block of tetraphenylmethane for removal of $Cr_2O_7^{2-}$ from wastewater. The ion exchange from Br^- to Cl^- afforded significant enhancement in $Cr_2O_7^{2-}$ adsorption performance for CPN-tpm-Cl, which can be attributed to the higher hydrophilicity and smaller ion radius of Cl^-. Our work not only contributes a facile and efficient approach to enhance the adsorption performance of cationic polymer towards $Cr_2O_7^{2-}$ by simply counter anion exchange, but also paves a way to develop cationic polymeric nanotraps as a new type of adsorbents for wastewater treatment.

CRediT authorship contribution statement

Xiaorui Li: Data curation, Formal analysis, Writing – original draft. **Linfeng Jin:** Data curation. **Lei Huang:** Data curation. **Xueying Ge:** Data curation. **Haoyu Deng:** Data curation. **Haiying Wang:** Data curation. **Yiming Li:** Conceptualization, Methodology, Supervision, Writing – review & editing. **Liyuan Chai:** Conceptualization, Methodology, Supervision, Writing – review & editing. **Shengqian Ma:** Conceptualization, Methodology, Supervision, Writing – review & editing.

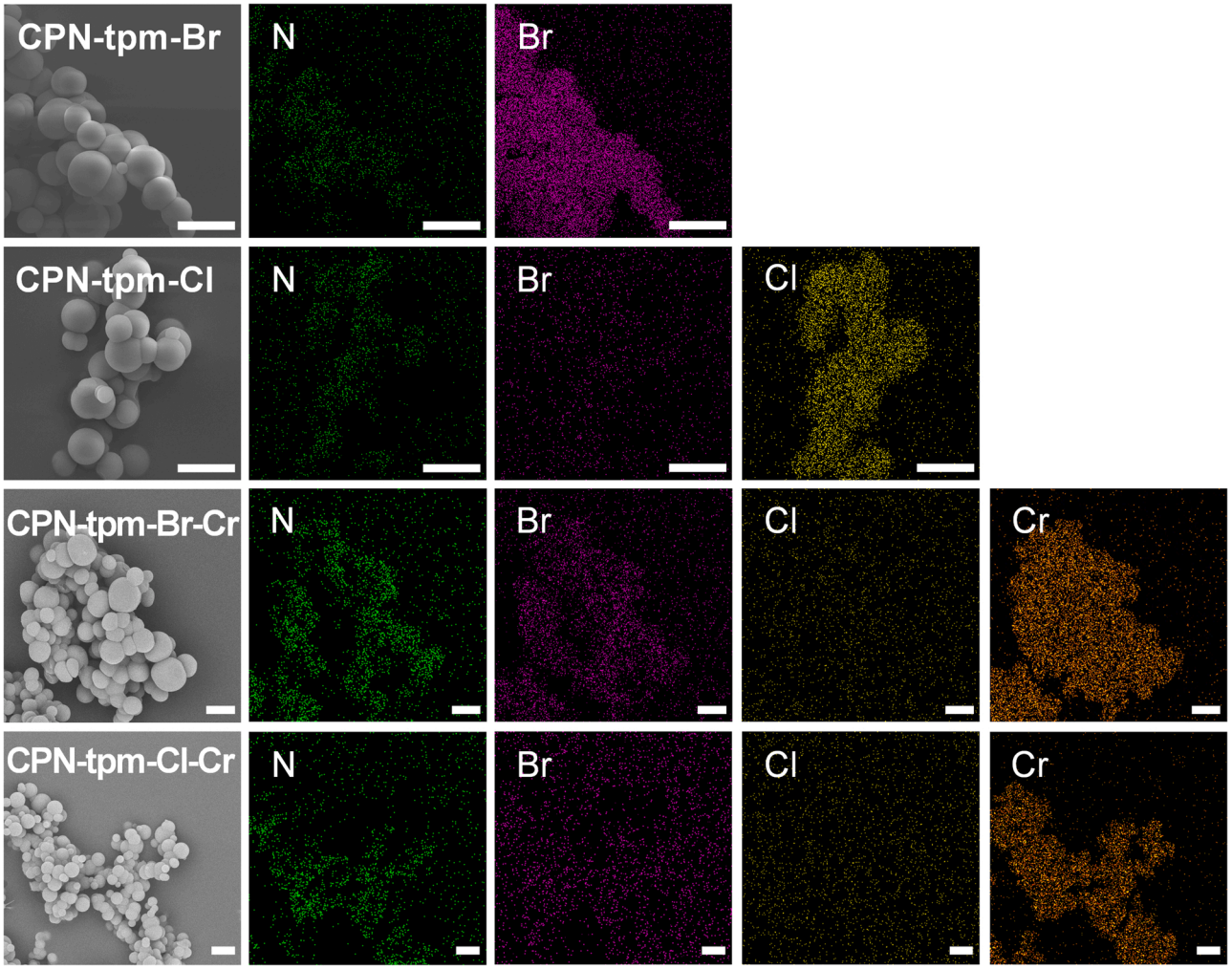

Fig. 8. SEM-EDS mapping of CPN-tpm-Br, CPN-tpm-Cl, CPN-tpm-Br-Cr and CPN-tpm-Cl-Cr.

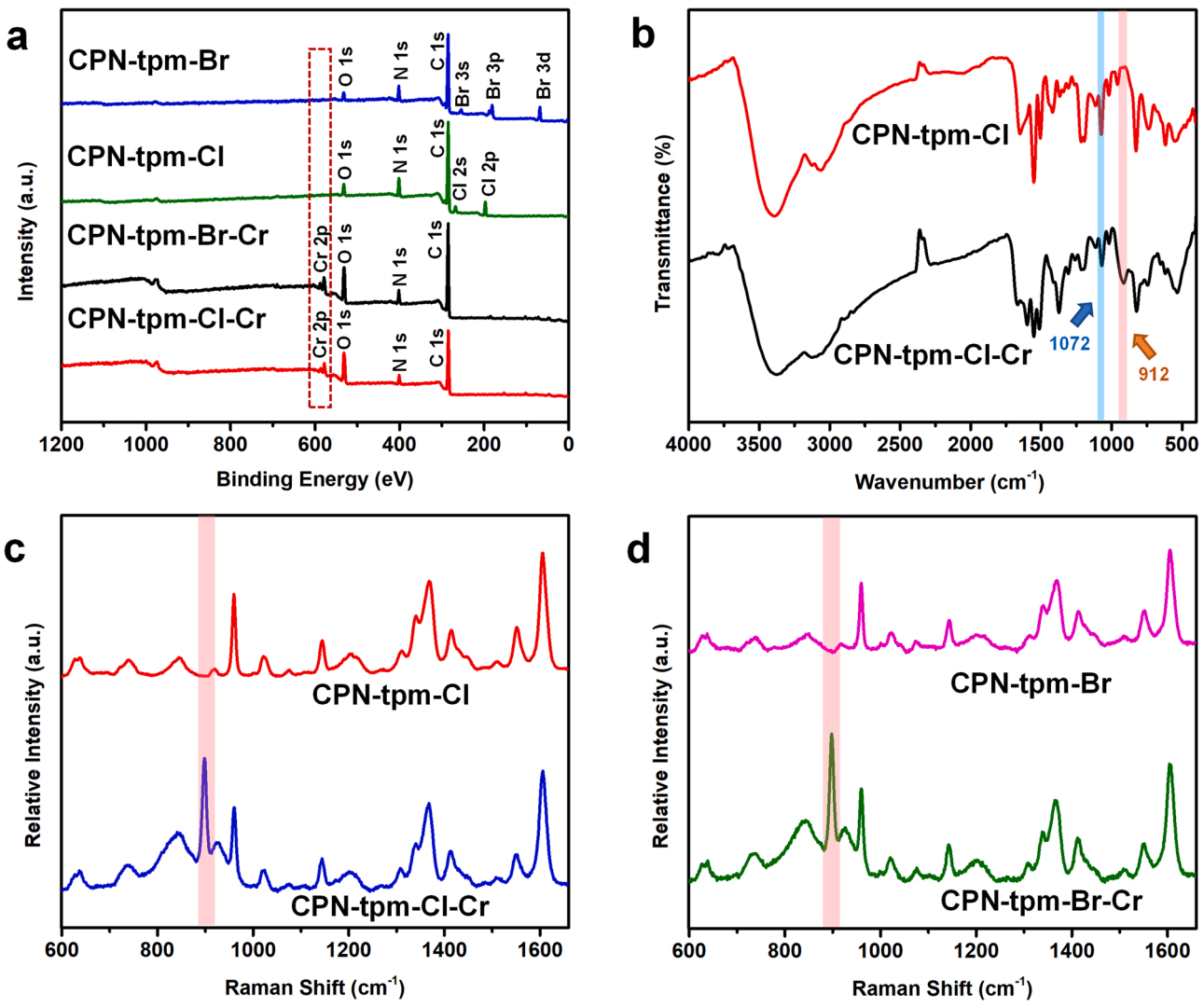

Fig. 9. a) The XPS survey spectra of CPN-tpm-Br, CPN-tpm-Cl, CPN-tpm-Br-Cr and CPN-tpm-Cl-Cr. b) FT-IR spectra of CPN-tpm-Cl before and after sorption with $Cr_2O_7^{2-}$. Raman spectra of c) CPN-tpm-Cl and d) CPN-tpm-Br before and after sorption with $Cr_2O_7^{2-}$.

Declaration of Competing Interest

The authors declare that they have no known competing financial interests or personal relationships that could have appeared to influence the work reported in this paper.

Acknowledgments

This work was supported by the National Key R&D Program of China (2018YFC1802204, 2020YFC1909200), National Natural Science Fund of China for Distinguished Young Scholars (51825403), Key R&D Program of Hunan Province (2018SK2026) and China Scholarship Council (CSC) (201706370186). Partial support from the U.S. National Science Foundation (CBET-1706025) and the Robert A. Welch Foundation (B-0027) is also acknowledged.

Appendix A. Supporting information

Supplementary data associated with this article can be found in the online version at doi:10.1016/j.jece.2021.106357.

References

[1] P. Samanta, P. Chandra, S. Dutta, A. Desai, S.K. Ghosh, Chemically stable ionic viologen-organic network: an efficient scavenger of toxic oxo-anions from water, Chem. Sci. 9 (2018) 7874–7881.
[2] Y.Q. Su, Y.X. Wang, X.J. Li, X.X. Li, R.H. Wang, Imidazolium-based porous organic polymers: anion exchange driven capture and luminescent probe of $Cr_2O_7^{2-}$, ACS Appl. Mater. Interfaces 8 (2016) 18904–18911.
[3] Y. He, S.I. Alhassan, W. Zhang, L. Hou, X. Chen, X. Li, B. Wu, Y. Zhao, L. Jin, L. Huang, H. Wang, Electrochemically-mediated capture and reduction of Cr(VI) by highly porous N-doped carbon spheres, J. Environ. Chem. Eng. 9 (2021), 106067.
[4] W. Jiang, M. Pelaez, D.D. Dionysiou, M.H. Entezari, D. Tsoutsou, K. O'Shea, Chromium(VI) removal by maghemite nanoparticles, Chem. Eng. J. 222 (2013) 527–533.
[5] A. Nagaraj, M.A. Munusamy, A.A. Al-Arfaj, M. Rajan, Functional ionic liquid-capped graphene quantum dots for chromium removal from chromium contaminated water, J. Chem. Eng. Data 64 (2018) 651–667.
[6] Y. Cao, J. Huang, Y. Li, S. Qiu, J. Liu, A. Khasanov, M.A. Khan, D.P. Young, F. Peng, D. Cao, X. Peng, K. Hong, Z. Guo, One-pot melamine derived nitrogen doped magnetic carbon nanoadsorbents with enhanced chromium removal, Carbon 109 (2016) 640–649.
[7] Y.X. Wang, H.X. Zhao, X.X. Li, R.H. Wang, A durable luminescent ionic polymer for rapid detection and efficient removal of toxic $Cr_2O_7^{2-}$, J. Mater. Chem. A 4 (2016) 12554–12560.
[8] Z.-J. Li, H.-D. Xue, Y.-Q. Zhang, H.-S. Hu, X.-D. Zheng, Construction of a cationic organic network for highly efficient removal of anionic contaminants from water, N. J. Chem. 43 (2019) 11604–11609.
[9] A.V. Desai, B. Manna, A. Karmakar, A. Sahu, S.K. Ghosh, A water-stable cationic metal-organic framework as a dual adsorbent of oxoanion pollutants, Angew. Chem. Int. Ed. 55 (2016) 7811–7815.

[10] X. Li, H. Xu, F. Kong, R. Wang, A cationic metal-organic framework consisting of nanoscale cages: capture, separation, and luminescent probing of $Cr_2O_7^{2-}$ through a single-crystal to single-crystal process, Angew. Chem. Int. Ed. 52 (2013) 13769–13773.
[11] X.X. Lv, L.L. Shi, K. Li, B.L. Li, H.Y. Li, An unusual porous cationic metal-organic framework based on a tetranuclear hydroxyl-copper(II) cluster for fast and highly efficient dichromate trapping through a single-crystal to single-crystal process, Chem. Commun. 53 (2017) 1864–1867.
[12] Y. Xie, J. Liang, Y. Fu, M. Huang, X. Xu, H. Wang, S. Tu, J. Li, Hypercrosslinked mesoporous poly(ionic liquid)s with high ionic density for efficient CO_2 capture and conversion into cyclic carbonates, J. Mater. Chem. A 6 (2018) 6660–6666.
[13] S. Fischer, A. Schimanowitz, R. Dawson, I. Senkovska, S. Kaskel, A. Thomas, Cationic microporous polymer networks by polymerisation of weakly coordinating cations with CO_2-storage ability, J. Mater. Chem. A 2 (2014) 11825–11829.
[14] H. Fang, S. Sun, P. Liao, Y. Hu, J. Zhang, Gold nanoparticles confined in imidazolium-based porous organic polymers to assemble a microfluidic reactor: controllable growth and enhanced catalytic activity, J. Mater. Chem. A 6 (2018) 2115–2121.
[15] Q. Sun, S. Ma, Z. Dai, X. Meng, F.-S. Xiao, A hierarchical porous ionic organic polymer as a new platform for heterogeneous phase transfer catalysis, J. Mater. Chem. A 3 (2015) 23871–23875.
[16] J. Yuan, S. Prescher, K. Sakaushi, M. Antonietti, Novel polyvinylimidazolium nanoparticles as high-performance binders for lithium-ion batteries, J. Mater. Chem. A 3 (2015) 7229–7234.
[17] J. Li, X. Dai, L. Zhu, C. Xu, D. Zhang, M.A. Silver, P. Li, L.H. Chen, Y.Z. Li, D. W. Zuo, H. Zhang, C.L. Xiao, J. Chen, J. Diwu, O.K. Farha, T.E. Albrecht-Schmitt, Z. F. Chai, S.A. Wang, $^{99}TcO_4^-$ remediation by a cationic polymeric network, Nat. Commun. 9 (2018) 3007.
[18] Y. Xie, J. Lin, H. Lin, Y. Jiang, J. Liang, H. Wang, S. Tu, J. Li, Removal of anionic hexavalent chromium and methyl orange pollutants by using imidazolium-based mesoporous poly(ionic liquid)s as efficient adsorbents in column, J. Hazard. Mater. 392 (2020), 122496.
[19] S.-Y. Zhang, W.-T. Gong, W.-D. Qu, X.-R. Deng, K.-X. Dong, S.-G. Zhang, G.-L. Ning, Construction of ionic porous organic polymers (iPOPs) via pyrylium mediated transformation, Chin. J. Polym. Sci. 38 (2020) 958–964.
[20] P. Zhang, Z.-A. Qiao, X. Jiang, G.M. Veith, S. Dai, Nanoporous ionic organic networks: stabilizing and supporting gold nanoparticles for catalysis, Nano Lett. 15 (2015) 823–828.
[21] Y. Xie, Q. Sun, Y. Fu, L. Song, J. Liang, X. Xu, H. Wang, J. Li, S. Tu, X. Lu, J. Li, Sponge-like quaternary ammonium-based poly(ionic liquid)s for high CO_2 capture and efficient cycloaddition under mild conditions, J. Mater. Chem. A 5 (2017) 25594–25600.
[22] X. Wei, R. Ma, T. Luo, Thermal conductivity of polyelectrolytes with different counterions, J. Phys. Chem. C 124 (2020) 4483–4488.
[23] Q. Sun, B. Aguila, Y. Song, S. Ma, Tailored porous organic polymers for task-specific water purification, Acc. Chem. Res. 53 (2020) 812–821.
[24] X. Li, Y. Li, H. Wang, Z. Niu, Y. He, L. Jin, M. Wu, H. Wang, L. Chai, A.M. Al-Enizi, A. Nafady, S.F. Shaikh, S. Ma, 3D cationic polymeric network nanotrap for efficient collection of perrhenate anion from wastewater, Small 17 (2021), 2007994.
[25] Y. Zhang, B. Aguila, S. Ma, Q. Zhang, Comparison of the use of functional porous organic polymer (POP) and natural material zeolite for nitrogen removal and recovery from source-separated urine, J. Environ. Chem. Eng. 8 (2020), 104296.
[26] Y. Byun, S.H. Je, S.N. Talapaneni, A. Coskun, Advances in porous organic polymers for efficient water capture, Chem. Eur. J. 25 (2019) 10262–10283.
[27] F.M. Wisser, K. Eckhardt, D. Wisser, W. Böhlmann, J. Grothe, E. Brunner, S. Kaskel, Tailoring pore structure and properties of functionalized porous polymers by cyclotrimerization, Macromolecules 47 (2014) 4210–4216.
[28] C. Chen, N.J. Feng, Q.R. Guo, Z. Li, X. Li, J. Ding, L. Wang, H. Wan, G.F. Guan, Surface engineering of a chromium metal-organic framework with bifunctional ionic liquids for selective CO_2 adsorption: synergistic effect between multiple active sites, J. Colloid Interf. Sci. 521 (2018) 91–101.
[29] S. Rapti, A. Pournara, D. Sarma, I.T. Papadas, G.S. Armatas, Y.S. Hassan, M. H. Alkordi, M.G. Kanatzidis, M.J. Manos, Rapid, green and inexpensive synthesis of high quality UiO-66 amino-functionalized materials with exceptional capability for removal of hexavalent chromium from industrial waste, Inorg. Chem. Front. 3 (2016) 635–644.
[30] D.X. Xue, F.J. Yu, Z.J. Zhang, Y. Yang, One-step synthesis of carbon dots embedded zincone microspheres for luminescent detection and removal of dichromate anions in water, Sens. Actuators B – Chem. 279 (2019) 130–137.
[31] H. Wang, H. Deng, Y. He, L. Huang, D. Wei, T. Hao, S. Wang, L. Jin, L. Zhang, Facile and sustainable synthesis of slit-like microporous N-doped carbon with unexpected electrosorption performance, Chem. Eng. J. 396 (2020), 125249.
[32] J.R. Keith, N.J. Rebello, B.J. Cowen, V. Ganesan, Influence of counterion structure on conductivity of polymerized ionic liquids, ACS Macro Lett. 8 (2019) 387–392.
[33] M. Ding, L. Chen, Y. Xu, B. Chen, J. Ding, R. Wu, C. Huang, Y. He, Y. Jin, C. Xia, Efficient capture of Tc/Re(VII, IV) by a viologen-based organic polymer containing tetraaza macrocycles, Chem. Eng. J. 380 (2020), 122581.
[34] W. Tao, H. Zhong, X. Pan, P. Wang, H. Wang, L. Huang, Removal of fluoride from wastewater solution using Ce-AlOOH with oxalic acid as modification, J. Hazard. Mater. 384 (2020), 121373.
[35] W.A. El-Mehalmey, A.H. Ibrahim, A.A. Abugable, M.H. Hassan, R.R. Haikal, S. G. Karakalos, O. Zaki, M.H. Alkordi, Metal-organic framework@silica as a stationary phase sorbent for rapid and cost-effective removal of hexavalent chromium, J. Mater. Chem. A 6 (2018) 2742–2751.
[36] T. Cremer, C. Kolbeck, K.R. Lovelock, N. Paape, R. Wolfel, P.S. Schulz, P. Wasserscheid, H. Weber, J. Thar, B. Kirchner, F. Maier, H.P. Steinruck, Towards a molecular understanding of cation-anion interactions–probing the electronic structure of imidazolium ionic liquids by NMR spectroscopy, X-ray photoelectron spectroscopy and theoretical calculations, Chem. Eur. J. 16 (2010) 9018–9033.
[37] I.J. Villar-Garcia, E.F. Smith, A.W. Taylor, F. Qiu, K.R. Lovelock, R.G. Jones, P. Licence, Charging of ionic liquid surfaces under X-ray irradiation: the measurement of absolute binding energies by XPS, Phys. Chem. Chem. Phys. 13 (2011) 2797–2808.
[38] C.P. Li, H. Zhou, J.J. Wang, B.L. Liu, S. Wang, X. Yang, Z.L. Wang, C.S. Liu, M. Du, W. Zhou, Mechanism-property correlation in coordination polymer crystals toward design of a superior sorbent, ACS Appl. Mater. Inter. 11 (2019) 42375–42384.
[39] X.F. Sun, Y. Ma, X.W. Liu, S.G. Wang, B.Y. Gao, X.M. Li, Sorption and detoxification of chromium(VI) by aerobic granules functionalized with polyethylenimine, Water Res. 44 (2010) 2517–2524.
[40] X. Liang, X. Fan, R. Li, S. Li, S. Shen, D. Hu, Efficient removal of Cr(VI) from water by quaternized chitin/branched polyethylenimine biosorbent with hierarchical pore structure, Bioresour. Technol. 250 (2018) 178–184.
[41] L. Li, D.Y. Kim, G.M. Swain, Transient formation of chromate in trivalent chromium process (TCP) coatings on AA2024 as probed by Raman spectroscopy, J. Electrochem. Soc. 159 (2012) C326–C333.